



International Commission on Illumination
Commission Internationale de l'Éclairage
Internationale Beleuchtungskommission

AN EXPERIMENTAL INVESTIGATION ON DEVELOPING A VISIBILITY MEASURE FOR THE PHANTOM ARRAY EFFECT FOR GENERAL LIGHTING APPLICATIONS

Kong, X., et al.

DOI 10.25039/x051.2025/dehqjf

This article is also published as part of:

Proceedings of the CIE 2025 Midterm Meeting Vienna, Austria, July 4-11, 2025:
Scientific Conference (July 7-9, 2025)

DOI 10.25039/x051.2025

in

Proceedings of the CIE (International Commission on Illumination)

ISSN no. 3061-015X (print), 3061-0168 (online)

The paper has undergone double-blind peer review and its final version has been presented at the CIE 2025 Midterm Meeting, Vienna, Austria, July 4–11, 2025.

© CIE 2025

All rights reserved. This work is licensed under the Creative Commons Attribution-NonCommercial 4.0 International License (<https://creativecommons.org/licenses/by-nc/4.0/>). Any mention of organizations or products does not imply endorsement by the CIE.

CIE Central Bureau
Babenbergerstrasse 9/9A
A-1010 Vienna, Austria
Tel.: +43 1 714 31 87
e-mail: ciecb@cie.co.at — www.cie.co.at

AN EXPERIMENTAL INVESTIGATION ON DEVELOPING A VISIBILITY MEASURE FOR THE PHANTOM ARRAY EFFECT FOR GENERAL LIGHTING APPLICATIONS

Kong, X.¹, Perz, M.², Heynderickx, I.¹

¹ Eindhoven University of Technology, Eindhoven, THE NETHERLANDS, ² Signify, Eindhoven, THE NETHERLANDS

x.kong@tue.nl

Abstract

The phantom array effect (PAE) has been extensively studied, but data on its visibility in well-illuminated environments, such as offices, remain insufficient for designing an appropriate visibility measure. According to CIE 249:2022, two essential sets of parameters are needed to develop such a measure: the temporal contrast threshold function and the Minkowski norm (i.e., the frequency summation exponent). Therefore, we designed an experiment to measure the visibility threshold of the PAE under the circumstances of a vertical illuminance of ~75 lx at eye level. In the experiment, we used sinusoidal waveforms at different frequencies, as well as complex waveforms, consisting of combinations of two or three sinusoids.

Keywords: Temporal Light Modulation, Temporal Light Artefact, The Phantom Array Effect, Visual Perception, General Lighting Applications

1 Introduction

The CIE 249:2022 publication (CIE, 2022) distinguishes three temporal light artifacts (TLAs): flicker, the stroboscopic effect, and the phantom array effect (PAE). Models that predict the visibility of flicker (e.g., the Flicker Visibility Measure (FVM), P_{st}^{LM} or M_p) and of the stroboscopic effect (i.e., the Stroboscopic Visibility Measure (SVM)) are described in literature (Perz et al., 2017, 2018; Perz, 2019; CIE, 2022); some have been adopted in research settings as well as in industrial practises, and have been standardized—for instance, through the inclusion in the EU Ecodesign Directive (European Union, 2009). Those visibility measures, however, have been defined using measurements in a specific *context*, and therefore are also only reliably applicable for this *context*. As such, the SVM was developed for general indoor applications with an average illuminance > 100 lx on the object of interest. Hence, for situations with an average illuminance <100 lx (relatively low lighting, roughly between candlelight and a shaded corner indoors), the parameters for the SVM are yet to be defined.

The phantom array effect is a visual phenomenon that occurs when a light source fluctuates in luminance or spectral distribution over time, and an observer moves their eyes rapidly (saccades) across it. Under these circumstances a stationary object can appear as a series of spatially separated replications of the object or a "phantom array." The PAE is particularly noticeable in low-light conditions (i.e., high contrast between light source and its surroundings), as occurring when observing LED vehicle taillights at night. Several variables influence the visibility of the PAE, including individual characteristics, characteristics of the light modulation, and characteristics of the viewing geometry.

Currently, no standardized model exists to predict the visibility threshold of the PAE. According to CIE 249:2022, two essential sets of parameters are needed to develop a visibility measure: the temporal contrast threshold function that defines the sensitivity, and the Minkowski norm that defines how various frequency components in a complex waveform are to be combined. Recently, Tan et al. (2024) provided this information and proposed a PAE visibility measure—the Phantom Array Visibility Measure (PAVM)—based on data collected by Miller et al. (2023), and using a general definition similar to that of SVM. However, we see two reasons for

extending this work: (1) the data of Miller et al. (2023) are not necessarily the most accurate representation of visibility thresholds, and (2) these data have been measured in a low light environment, which may not be representative for general lighting applications.

With respect to the first point, PAVM is derived from visibility thresholds measured for different waveforms using rating scores, ranging from 0: no pattern visible, to 6: highly visible pattern. The visibility threshold is then defined as the modulation corresponding to a rating score of 1 (Miller et al., 2023). Scores on such rating scales, however, are known to be prone to subjective interpretation of the scale, and people tend to spread stimuli over the mid-part of a rating scale independent of the actual content of the stimuli (Podsakoff et al., 2003). As a consequence, scores on rating scales are not the most accurate method for determining visibility thresholds. Paired comparisons, on the other hand, are generally more robust, as they leverage the human visual system's natural strength of relative judgment (e.g., Thurstone, 1927). In addition, the presence of a reference stimulus further enhances this reliability by anchoring perception and reducing inter-individual variability. Results of multiple comparisons are combined into a psychometric function, relating stimulus strength to the probability of its detection. A particular threshold point (e.g., the 75 % correct performance level) can then be derived from this function, or with the use of adaptive methods such as QUEST+ (Watson, 2017) that allow efficient convergence of the stimuli modulation to such a threshold point.

With respect to the second point, the light source used in Tan et al. (2024) had a luminance of 38 700 cd·m⁻² and subtended a visual angle of 0,06° when viewed by the participants at a distance of 3 m. The total illuminance at the eye was 1,6 lx, including about 1 lx from the light source itself. As such, the PAVM is designed for low-light situations. It is unlikely to be adequate for general indoor applications with a higher illuminance, since the adaptation state of the observer influences both the temporal and spatial sensitivity (e.g., Barten, 1993; Rider et al., 2016). So, to develop the visibility of the PAE for general lighting applications, a higher vertical illuminance at the eye than that used in the literature (i.e., 1,6 lx in Tan et al., 2024; <1 lx in Kong et al., 2023, 2025; <1 lx Kang et al., 2023) is needed.

Therefore, we designed an experiment to measure the visibility threshold of the PAE at various frequencies under the condition of a vertical illuminance at the eye of ~75 lx, using a paired-comparison based method.

2 Methods

The experiment consisted of a two-alternative forced-choice (2AFC) task. The stimulus was generated by two vertically aligned light sources, which were placed behind two thin vertical slits made from a black foam board. Both light sources had the identical size of 0,3 cm (width) × 4,3 cm (height), one positioned on top of the other with an in-between distance of 2 cm. Both light sources had a luminance of 10 000 cd·m⁻² and subtended a visual angle of 0,17° (horizontally) × 2,5° (vertically) when being viewed at a distance of 1 m. One light source was the reference driven with a direct current (DC), while the other was the test stimulus, driven by a sinusoidally modulated or complex waveform.

Four non-luminous stickers (i.e., Ø=2 cm)—two located in the middle of the height of the top light source, one at each side and 62 cm apart; two located in the middle of the height of the bottom light source, again one at each side and 62 cm apart—were provided as visual guides to facilitate the participants making 34,5-degree saccades across both light sources. Their task was to indicate in which of the two light sources they observed the PAE.

The experiment consisted of two sessions. In the first session, a Bayesian adaptive psychophysical procedure QUEST+ (Watson, 2017), implemented as a MATLAB Toolbox (Brainard, 2017), was used to change the modulation depth (*MD*) of the sinusoidal waveforms. This modulation depth is defined as the Michelson contrast:

$$MD = \frac{L_{max} - L_{min}}{L_{max} + L_{min}} \times 100\% \quad (1)$$

with L_{max} and L_{min} being the maximum and minimum luminance in the waveform, respectively. In the second session, the QUEST+ method was used to change the *MD* of complex waveforms, which were generated based on the results from the first session and consisted of combinations

of two or three sinusoidal waveforms at different frequencies. The resulting data expressed as *MD*, varying between 0 (i.e., DC light) and 100 %, were fitted to determine the visibility threshold.

2.1 Experimental Setup

The experimental setup is shown in Figure 1. Light was provided through a customized luminaire which consisted of 2 rows of LUXEON Rebel LEDs with a CCT of 6 500 K, positioned in a vertical plane. A customized diffuser and a neutral density (ND) filter with a transmission percentage of about 43 % were placed in front of the luminaire to improve uniformity. To control the light output (i.e., temporal frequency, modulation depth and shape), a programmable waveform generator (KEYSIGHT Agilent 33522B Series) was used and controlled via TCP/IP protocol by a laptop running MATLAB R2024a. An electronic load (Agilent N3300A) was used to drive the LEDs. Each light source was calibrated with the JETI Specbos 1201 spectroradiometer from 0 to 4 V in steps of 50 mV. A third-order polynomial function was used to build the inverse relation for each light source to ensure a proper transfer from voltage to luminance. This resulted in a goodness-of-fit of 0.99 for each light source.

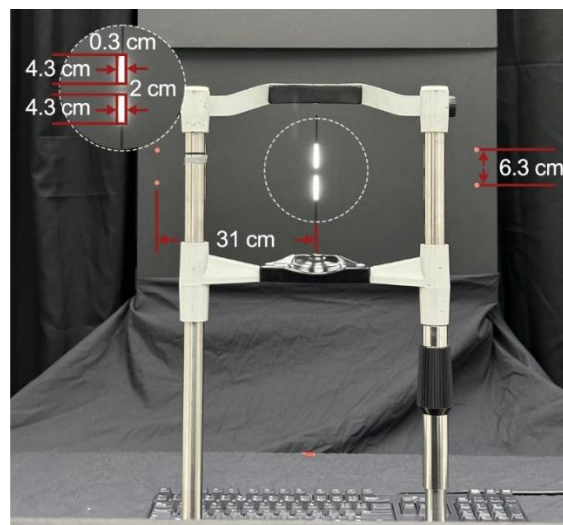


Figure 1 – Experimental setup. The stimulus consisted of two $0,17^\circ$ (horizontally) \times $2,5^\circ$ (vertically) light sources, which were controlled independently, separated by a gap of 2 cm.

The ceiling of the laboratory was equipped with sixteen lighting fixtures (Philips Savio TPS760 C), consisting of two types of fluorescent tubes: with a warm-white CCT (2700 K) and a cool-white CCT (6500 K). During the experiment, only the cool-white light was used. The ceiling light fixtures were adjusted via an in-house control interface in such a way that the horizontal illuminance on the table surface was between 255 lx and 335 lx. The vertical illuminance at the participants' eye level (i.e., 1,2 m above the ground) was measured to be about 75 lx. During the experiment, the ceiling light remained constant.

2.2 Stimuli

The modulated light source (stimulus) and the DC-driven reference had a time-averaged luminance of $10\,000\text{ cd}\cdot\text{m}^{-2}$. The position (top or bottom) of the reference and of the stimulus was randomized and balanced such that the stimulus appeared at the top in 50 % of all trials.

2.3 Procedure

The experimental protocol was approved by the Ethical Review Board (ERB) of the Human-Technology Interaction Group of the Eindhoven University of Technology. Participants were recruited through courses, and from the experimenters' network. The selection criteria were aged above 18 years with no history of migraine or epilepsy. The recruited participants were welcomed to the laboratory and then instructed to read and sign the informed consent form, under the constant room illumination described above. The participant's age and gender were collected as well.

2.3.1 Explanation of the PAE and the task

The participants were seated in front of the experimental set-up, were given an explanation about the PAE, and were provided with instructions for the experiment. Participants were asked to make for each trial at least three rapid horizontal saccades between the two non-luminous stickers across the top light source, and then at least three rapid horizontal saccades across the bottom light source. Then they could press the *up arrow* key to indicate that the PAE was observed in the light source on top, or the *down arrow* key to indicate that the PAE was observed in the light source at the bottom. If they couldn't detect the PAE, they were instructed to press either key (i.e., to guess). The participants were facilitated with audio cues, i.e., a *beep* sound which indicated the start of a new trial, and other computer-generated voice instructions such as "Input recorded", and "Invalid input, please input again".

To demonstrate the occurrence of the PAE, we choose a pair of stimuli—a reference stimulus of DC and a PAE stimulus consisting of a complex waveform composed of a sinusoid of 100 Hz and a sinusoid of 600 Hz, at a modulation depth of 96 %. Earlier trials had demonstrated that the PAE is visible for most observers under this condition. It was indicated to the participants that the PAE could be observed either in the top or bottom light source. In addition, two DC stimuli were presented simultaneously to illustrate that the task could be difficult in which case participants would be forced to make a guess.

When the participants had no further questions, the four practice trials started. They consisted of paired comparisons between the stimulus used during the instruction phase and DC. Participants who did not identify the four practice trials 100 % *correctly*, even after additional explanation and practice, were excluded from further participation, and were financially compensated for the efforts to come to the lab.

2.3.2 Data collection

The experiment was divided into two sessions, which are described in detail below. In the first session, the visibility thresholds of sinusoidal waveforms at five frequencies were measured in an intermingled order. After all trials in Session 1 were finished, the participant was given a short break during which the visibility thresholds were computed for further use in Session 2. This second session measured the visibility threshold of complex waveforms, for which two or three sinusoids at different frequencies were combined at their respective threshold modulation per participant. After the second session was finished, the participants were debriefed about the design and purpose of the experiment. Afterwards, they received financial compensation.

2.3.3 Session 1: Determination of the contrast threshold function

In the first session, we measured the visibility threshold to the PAE using waveforms sinusoidally modulated in luminance at five frequencies: 100 Hz, 600 Hz, 1 200 Hz, 1 800 Hz, and 3 600 Hz. The modulation depth as expressed in Equation (1) was transformed to a logarithm scale (i.e., in dB) for its use in the QUEST+ method (Watson, 2017); hence we used:

$$s_i = 20 \times \log_{10}(MD_i) \quad (2)$$

with MD_i representing the i -th stimulus in linear space (defined in Equation (1)), and s_i representing the i -th stimulus in dB.

For each frequency and participant, a Weibull cumulative distribution function was fitted to the data using the maximum likelihood method (MATLAB toolbox; Brainard, 2017) to estimate the psychometric function. The Weibull function is defined as:

$$q = 1 - \lambda + (\gamma + \lambda - 1) \cdot e^{-10^{(\beta \cdot s - \alpha)/20}} \quad (3)$$

where

q	is the proportion of correct responses (ranging from 0 to 1);
λ	is the lapse rate, fixed at 0,02, accounting for a 2 % probability of accidental errors;
γ	is the guessing rate, fixed at 0,5 for the 2AFC task (50 % chance level);
β	is the slope of the psychometric function, fixed at 3;
s	is the stimulus intensity (modulation depth in dB);
α	is the estimated threshold in dB, corresponding to the stimulus intensity required for 75 % correct performance.

The visibility threshold (α) is defined as the intensity level yielding 75 % correct responses, which is the mid-point between the 50 % chance level (guessing) and the certainty level of 100 % in this 2AFC paradigm. If $\alpha_p^{(k)}$ represents the visibility threshold (in dB) for participant p at frequency f_k of the sinusoidal waveform, the visibility threshold expressed in linear space $\alpha_{lin,p}^{(k)}$ becomes (using Equation (2)):

$$\alpha_{lin,p}^{(k)} = 10^{\alpha_p^{(k)}/20} \tag{4}$$

2.3.4 Session 2: Determination of the Minkowski summation exponent

In the second session, we used four complex waveforms, generated by combining two or three sinusoidal waveforms at the threshold modulation per participant. Those four frequency combinations were: 1) 100 Hz + 600 Hz; 2) 600 Hz + 1200 Hz; 3) 1200 Hz + 1800 Hz; and 4) 600 Hz + 1200 Hz + 1800 Hz.

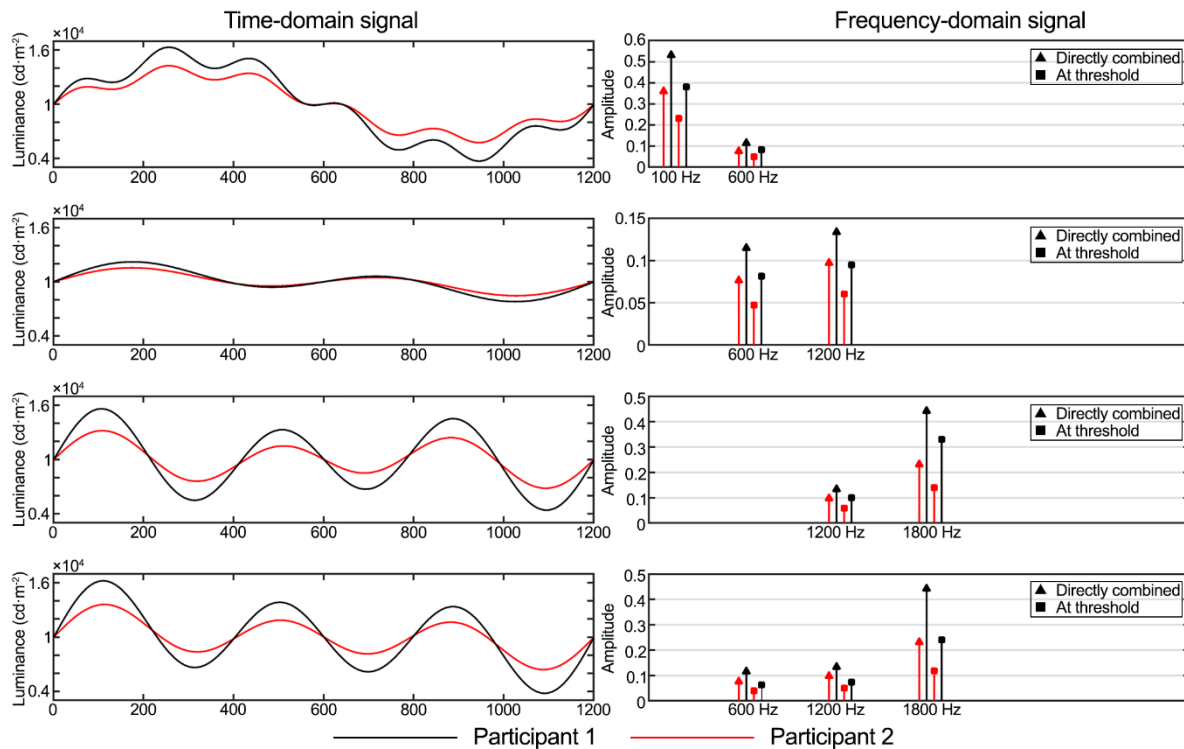


Figure 2 – (left) Complex waveforms generated using the visibility thresholds of two participants from Session 1. The four waveforms are used in Session 2 of the experiment. (right) The four waveforms expressed in the frequency domain using the Fourier transform. The ▲-datapoints represent the amplitudes when directly combining the waveforms at the respective visibility thresholds, while the ■-datapoints represent the amplitudes of the complex waveforms at their visibility threshold measured in Session 2 (see results).

The luminance waveform for a particular participant p and a particular frequency combination c is given as:

$$L_p^{(c)}(t) = L_0 \left[1 + \frac{1}{n_c} \sum_{j=1}^{n_c} \alpha_{lin,p}^{(k_j)} \cdot \sin(2\pi f_{k_j} t) \right] \tag{5}$$

where

- L_0 is the constant (temporally averaged) luminance level of 10 000 cd·m⁻²;
- n_c is the number of frequencies in the set: $\mathcal{F}^{(c)} = \{f_{k_1}, f_{k_2}, \dots, f_{k_{n_c}}\}$;
- k_j is the j -th component in $\mathcal{F}^{(c)}$.

The MD of this complex luminance waveform for participant p , denoted as $MD_p^{(c)}$, can be computed using Equation (1). Subsequently, QUEST+ in combination with Equations (3) and (4) allow to determine the visibility threshold $\alpha_{lin,p}^{(c)}$ of the complex waveform c . For two participants, the resulting waveforms (one cycle, consisting of 1 200 sample points) are shown in Figure 2 (left).

2.4 Participants

Forty-one participants (17 male and 24 female), aged between 19 and 62 years old (28 ± 9 years) signed up for the experiment. The majority (i.e., 36) of the participants had no prior knowledge about the PAE, and therefore were considered as naïve participants for the purpose of this study. Ten naïve participants (2 male and 8 female), aged between 19 and 30 years old (24 ± 4) did not start the actual data collection because they could not reliably identify the PAE during the practice trials. The rest of the 31 participants (15 male, 16 female), aged between 20 and 62 years old (29 ± 10), continued with the experiment. Among the 31 participants, one decided to quit the experiment after Session 1 due to visual discomfort.

3 Results

Based on the procedure, 155 (31 participants \times 5 frequencies) visibility thresholds to the PAE were obtained from Session 1, and 120 (30 participants \times 4 complex waveforms) visibility thresholds to the PAE were obtained from Session 2.

3.1 The visibility thresholds from data in Session 1 and Session 2

The visibility thresholds of Session 1 are visualized with a box plot in Figure 3. In line with existing literature, the mean visibility threshold shows a band-pass behaviour as a function of frequency, also at the ambient illumination level of 75 lx. Peak sensitivity (i.e., lowest visibility threshold) is around 600-1 000 Hz. Similarly, the visibility thresholds of Session 2 are visualized with a box plot in Figure 4.

3.2 The Minkowski summation exponents

Using a similar approach to the development of SVM (Perz et al., 2015) and following the recommended frequency-domain analysis in CIE 249:2022, the visibility measure that translates any input luminance waveform into a single number can be expressed as:

$$M_{PAE} = \sqrt[n]{\sum_{i=1}^{\infty} \left(\frac{A_i}{\alpha_{lin,i}}\right)^n} \begin{cases} < 1 & \text{not visible} \\ = 1 & \text{just visible} \\ > 1 & \text{visible} \end{cases} \quad (6)$$

where

A_i	is the amplitude of the i -th Fourier component of the luminance waveform divided by the DC component of the waveform;
$\alpha_{lin,i}$	is the visibility threshold of the sinusoidal waveform at the respective frequency;
n	is the Minkowski exponent.

The Minkowski exponent indicates how the frequency components of a complex waveform are summed or, in other words, how different frequency components in a complex waveform contribute to the visibility of the PAE. The parameter n determines the type of vector norm applied: when $n = 1$, the norm reduces to the Manhattan (\mathcal{L}^1) case, characterized by a linear summation of all frequency components. At $n = 2$, the formulation aligns with the conventional Euclidean (\mathcal{L}^2) norm. As $n \rightarrow \infty$, the norm converges to the Chebyshev (\mathcal{L}^∞) condition, wherein the visibility of the PAE is governed exclusively by the frequency component with the highest amplitude.

The Minkowski exponent is calculated from the scaling factors (κ) between the threshold modulation of the direct combination of sinusoidal waveforms (\blacktriangle -datapoints in Figure 2) and the threshold modulation of the combined waveforms (\blacksquare -datapoints in Figure 2). Figure 2 shows that the amplitude of the complex waveforms should be decreased to make the PAE just detectable. For waveforms 1 to 3, two scaling factors per waveform and participant could be computed, more specifically per contributing frequency one can calculate the ratio between the

amplitude of the Fourier component of the directly combined waveform over the waveform at threshold. Analogously, for waveform 4, three scaling factors can be computed per participant, i.e., one per contributing frequency. By design, these scaling factors in the frequency-domain are identical to the ratios in modulation depth. Hence, the scaling factor for participant p and waveform c can be computed as follows:

$$K_p^{(c)} = \frac{\alpha_{lin,p}^{(c)}}{MD_p^{(c)}} \tag{7}$$

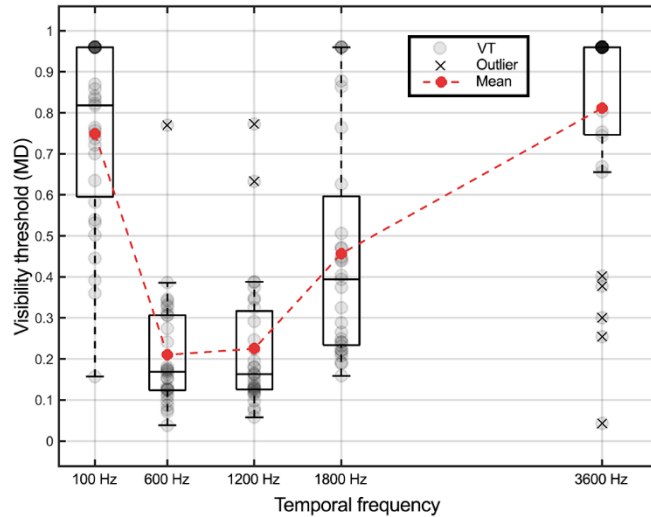


Figure 3 – Box plot of the visibility thresholds obtained in Session 1. The x-axis represents the temporal frequencies in Hz while the y-axis represents the visibility thresholds in modulation depth. The grey circular points represent the visibility thresholds for each individual participant, and the red points represent the mean visibility thresholds at each temporal frequency. Outliers are marked as x.

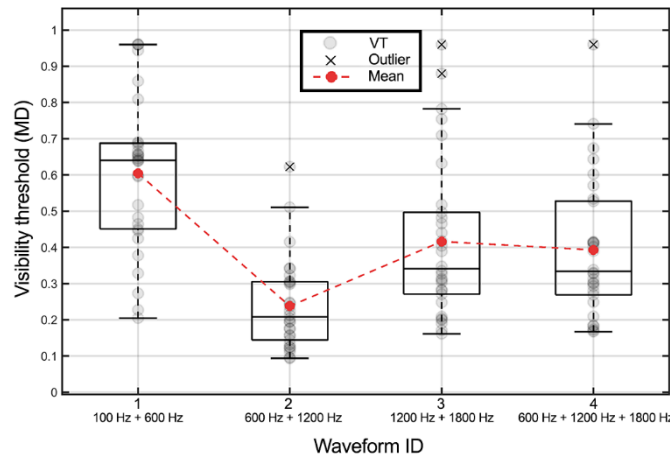


Figure 4 – Box plot of the visibility thresholds obtained in Session 2. The x-axis represents the waveform ID while the y-axis represents the visibility thresholds in modulation depth. The grey circular points represent the visibility thresholds for each participant, and the red points represent the mean visibility thresholds for each complex waveform. Outliers are marked as x.

In case the modulation at the PAE visibility threshold of the complex waveform is equal to the modulation resulting from combining multiple waveforms at their respective threshold modulation, the scaling factors at the various contributing frequencies would be 1. In that case the ▲-datapoints and the ■-datapoints in Figure 2 would be equal. Figure 2, however, already showed—based on the results of two participants—that the ■-datapoints are lower than the ▲-datapoints, which means that the modulation at the PAE visibility threshold of the complex

waveform is smaller than the modulation resulting from combining multiple waveforms at their respective threshold modulation. This implies that the scaling factors will be smaller than 1. In that case, adding more frequencies in the complex waveform is expected to reduce the actual scaling factors more.

The scaling factors of the four complex waveforms used in Session 2 were computed using Equation (7) and the results are visualized in Figure 5. As can be seen in this figure, the scaling factors of waveform 4, combining three sinusoidal waves, are smaller than the scaling factors of waveforms 1 to 3, combining only two sinusoidal waves. In addition, Figure 5 shows that most scaling factors are indeed smaller than 1. There are some exceptions; of the 120 (= 30 participants \times 4 complex waveforms) scaling factors, 6 were larger than 1.

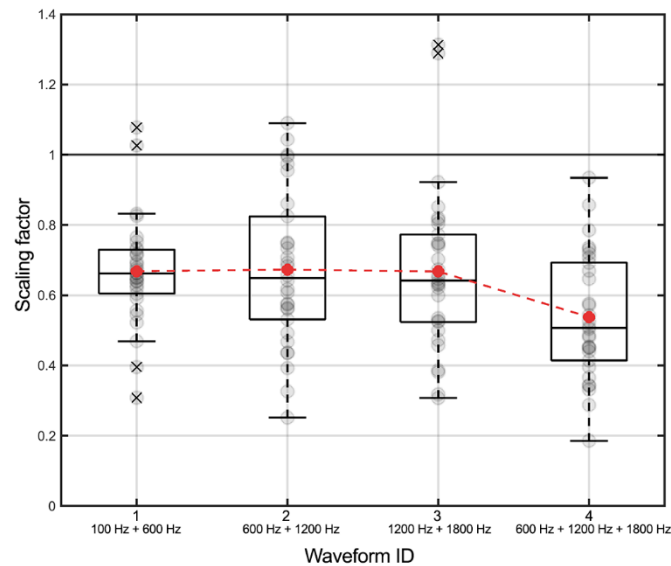


Figure 5 – Box plot of the scaling factors between the PAE threshold modulation of a complex waveform and the modulation resulting from combining multiple simple sinusoidal waveforms at threshold. The x-axis represents the waveform ID of the complex waveform. The y-axis represents the scaling factors as calculated with Equation (7). The grey circular points represent the scaling factor per participant, and the red points represent the mean scaling factor of each complex waveform. Outliers are marked as x.

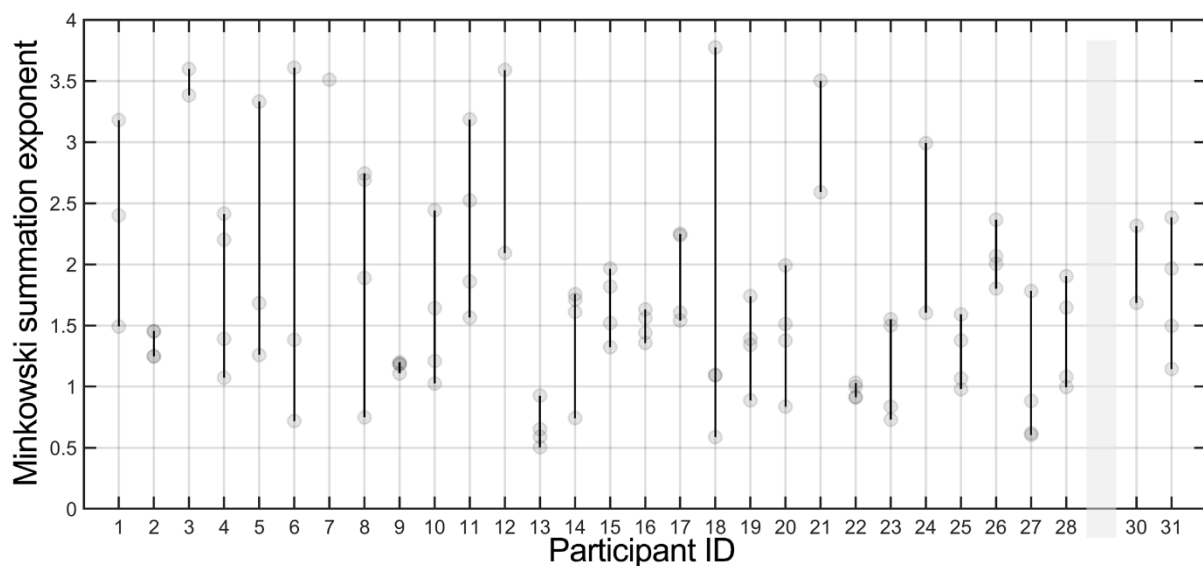


Figure 6 – The Minkowski summation exponents computed using Equation (8). The grey circular points represent the exponents for the four different complex waveforms per participant. Missing grey circular points are related to scaling factors, being larger than 1.

The Minkowski summation exponent n can now be computed from these scaling factors using the following simplified version of Equation (6):

$$\sqrt[n]{n_c \cdot (\kappa_p^{(c)})^n} = 1 \quad (8)$$

where $\kappa_p^{(c)}$ is defined in Equation (7), and n_c is 2 (i.e., two frequency components) for waveforms 1 to 3, and n_c is 3 (i.e., three frequency components) for waveform 4.

We determined the Minkowski summation exponent with Equation (8) per complex waveform and participant. As mentioned above, one participant (i.e., Participant 29) only finished Session 1, so this participant's Minkowski summation exponents are missing. The remaining 104 exponents (i.e., excluding the six data for which the scaling factor was larger than 1) are visualized in Figure 6. Averaging these 104 Minkowski summation exponents resulted in a value of 1,7, with a standard deviation of 0,8. The maximum value was 3,8, while the minimum value was 0,5.

4 Conclusion and discussion

We measured the visibility to the PAE under lighting levels which are more common, though still relatively low in real-life offices, i.e., with a horizontal illuminance of around 300 lx at the table and a vertical illuminance of about 75 lx at the eyes of the participant. We also used a very bright (time-averaged luminance of 10 000 cd·m⁻²) small (subtended angle of 0,17° horizontally) stimulus to realistically maximize the chance of seeing the PAE, while such light sources are not really common in daily life offices. Under these circumstances, the PAE sensitivity curve shows a bandpass shape with a maximum sensitivity of around 600-1 000Hz, in line with existing literature (CIE, 2022; Miller et al., 2023; Tan et al., 2024; Kong et al., 2023, 2025;). The modulation depth at maximum sensitivity is higher than what we found in our earlier experiments (Kong et al., 2023, 2025), but that could be expected with the higher ambient light.

Despite a few older participants, we used relatively young participants (mainly students), who are expected to be more sensitive to TLA (Veitch and Miller, 2024). Still, 10 out of the 41 young participants, roughly 25 % of the population, were not able to consistently perceive the PAE. These participants were excluded from our experiment, and as a consequence, the visibility thresholds we measured are lower (in terms of in modulation depth) than the thresholds that would be expected in an averaged population.

The Minkowski summation exponent we found is on average 1,7, which is—given the spread in data—reasonably close to the 2,1 value, reported by Tan et al. (2024). Considering the different environmental conditions and luminance of the light source we used in our experiment compared to Tan et al. (2024), it seems that the Minkowski summation exponent may be consistent across the different lighting *contexts*. This does not imply that the actual modulation thresholds are also independent of the specific lighting *context*. On the contrary, we do agree with all factors mentioned in the CIE 249:2022 document that affect the visibility threshold of the TLA. More specifically, we here chose one luminance level of the light source with one luminance level of the background, which most closely resembles conditions of a typical office; a more accurate estimation of the effect of both variables on the visibility of the PAE needs further research.

5 Acknowledgements

This study was jointly supported by the Human-Technology Interaction (HTI) group at Eindhoven University of Technology (TU/e) and Signify Research, the Netherlands. The authors would like to thank Nikolina Molnar, Sebastiaan Mulder, and Nasir Abed from the lab support team at TU/e, for their assistance with the experimental setup.

References

BARTEN, P.G. 1993. Spatiotemporal Model for the Contrast Sensitivity of the Human Eye and Its Temporal Aspects. In: *Human Vision, Visual Processing, and Digital Display IV*, 8 September, 1993, San Jose, United States. SPIE, 2-14. <https://doi.org/10.1117/12.152690>.

- BRAINARD, D.H. 2017. mQUESTPlus: A MATLAB Implementation of QUEST+. <https://github.com/brainardlab/mQUESTPlus>.
- CIE 2022. CIE 249:2022. Visual Aspects of Time-Modulated Lighting Systems. Vienna: CIE. <https://doi.org/10.25039/TR.249.2022>.
- EUROPEAN UNION 2009. Directive 2009/125/EC of the European Parliament and of the Council of 21 October 2009 Establishing a Framework for the Setting of Ecodesign Requirements for Energy-related Products. *Official Journal of the European Union*, L 285, 10-35. <http://data.europa.eu/eli/dir/2009/125/oj>.
- KANG, H.R., LEE, C.S., LEE, J.M. and LEE, K.M. 2023. Phantom Array Effect Can Be Observed Above 15 KHz in High Speed Eye Movement Group for High Luminance Warm White LED. *Lighting Res. Technol.*, 56(7), 669-675. <https://doi.org/10.1177/14771535221147312>.
- KONG, X., MARTINSONS, C., TENGELIN, M.N. and HEYNDERICKX, I. 2025. Measuring the Temporal Contrast Sensitivity Function of the Phantom Array Effect. *Lighting Res. Technol.*, Under review.
- KONG, X., VOGELS, R., MARTINSONS, C., TENGELIN, M.N. and HEYNDERICKX, I. 2023. Dependence of Temporal Frequency and Chromaticity on the Visibility of the Phantom Array Effect. In: *Proceedings of the 30th Session of the CIE*, 15-23 September, 2023, Ljubljana, Slovenia. Vienna: CIE, 347-356. <https://doi.org/10.25039/x50.2023.OP060>.
- MILLER, N.J., RODRIGUEZ-FEO BERMUDEZ, E., IRVIN, L. and TAN, J. 2023. Phantom Array and Stroboscopic Effect Visibility Under Combinations of TLM Parameters. *Lighting Res. Technol.*, 56(7), 707-733. <https://doi.org/10.1177/14771535231169904>.
- PERZ, M., VOGELS, I., SEKULOVSKI, D., WANG, L., TU, Y. and HEYNDERICKX I. 2015. Modeling the Visibility of the Stroboscopic Effect Occurring in Temporally Modulated Light Systems. *Lighting Res. Technol.*, 47(3), 281-300. <https://doi.org/10.1177/1477153514534945>.
- PERZ, M., SEKULOVSKI, D., VOGELS, I. and HEYNDERICKX, I. 2017. Quantifying the Visibility of Periodic Flicker. *LEUKOS: Journal of Illuminating Engineering Society of North America*, 13(3), 127-142. <https://doi.org/10.1080/15502724.2016.1269607>.
- PERZ, M., SEKULOVSKI, D., VOGELS, I. and HEYNDERICKX, I. 2018. Stroboscopic Effect: Contrast Threshold Function and Dependence on Illumination Level. *J. Opt. Soc. Am. A*, 35(2), 309-319. <https://doi.org/10.1364/JOSAA.35.000309>.
- PERZ, M. 2019. Modelling Visibility of Temporal Light Artefacts. Ph.D. Thesis. Eindhoven University of Technology. https://pure.tue.nl/ws/files/114194362/20190205_Perz.pdf.
- PODSAKOFF, P.M., MACKENZIE, S.B., LEE, J.Y. and PODSAKOFF, N.P. 2003. Common Method Biases in Behavioral Research: a Critical Review of the Literature and Recommended Remedies. *J. Appl. Psychol.*, 88(5), 879-903. <https://doi.org/10.1037/0021-9010.88.5.879>.
- RIDER, A., HENNING, B. and STOCKMAN, A. 2016. Light Adaptation and the Human Temporal Response Revisited. *J. Vision*, 16(12), 387-387. <https://doi.org/10.1167/16.12.387>.
- TAN, J., MILLER, N.J., ROYER, M.P. and IRVIN, L. 2024. Temporal Light Modulation: A Phantom Array Visibility Measure. *Lighting Res. Technol.*, 56(7), 772-789. <https://doi.org/10.1177/14771535241239611>.
- THURSTONE, L.L. 1927. A Law of Comparative Judgment. *Psychol. Rev.*, 34(4), 273-286. <https://doi.org/10.1037/h0070288>.
- VEITCH, J.A. and MILLER, N.J. 2024. Effects of Temporal Light Modulation on Individuals Sensitive to Pattern Glare. *LEUKOS: Journal of Illuminating Engineering Society of North America*, 20(3), 310-346. <https://doi.org/10.1080/15502724.2023.2299210>.
- WATSON, A.B. 2017. QUEST+: A General Multidimensional Bayesian Adaptive Psychometric Method. *J. Vision*, 17(3):10, 1-27. <https://doi.org/10.1167/17.3.10>.